Inorganica Chimica Acta 395 (2013) 176–180

Contents lists available at SciVerse ScienceDirect

Inorganica Chimica Acta

journal homepage: www.elsevier.com/locate/ica

Magnetic properties of vanadium(IV)-based extended systems: $[(VO)_3(\mu\text{-}PO_4)_2(2,2'\text{-bpy})(\mu\text{-}OH_2)]\cdot 1/3H_2O$ and $(VO)_2H_4P_2O_9$

D. Venegas-Yazigi [a,b,*], K. Muñoz [a], M. Saldías [b,c], K. Valdés de la Barra [a], A. Vega [b,d], V. Paredes-García [b,d], C.J. Gómez-García [e], E. Le Fur [f,g], W. Cañón-Mancisidor [b,h], E. Spodine [b,h]

[a] Facultad de Química y Biología, Universidad de Santiago de Chile (USACH), Chile
[b] Av. Alameda 3363, Estación Central, Santiago, Chile
[c] Facultad de Ciencias Físicas y Matemáticas, Universidad de Chile, Santiago, Chile
[d] Departamento de Ciencias Químicas, Universidad Andrés Bello, Chile
[e] Instituto de Ciencia Molecular, Parque Científico, Universidad de Valencia, C/ Catedrático José Beltrán 2, 46980 Paterna, Spain
[f] ENSCR, CNRS, UMR 6226, Rennes, France
[g] Université Européenne de Bretagne, France
[h] Facultad de Ciencias Químicas y Farmacéuticas, Universidad de Chile, Santiago, Chile

ARTICLE INFO

Article history:
Received 30 March 2012
Received in revised form 26 September 2012
Accepted 5 October 2012
Available online 3 November 2012

Keywords:
VPO
Hybrid materials
Molecular magnetism
Vanadium
DFT

ABSTRACT

The magnetic properties of $[(VO)_3(\mu\text{-}PO_4)_2(2,2'\text{-bpy})(\mu\text{-}OH_2)]1/3H_2O$ (**1**) and $(VO)_2H_4P_2O_9$ (**2**), a tubular and a layered vanadium(IV) phosphates containing triply oxido bridged V^{IV} dimers, are analyzed considering the Bleaney–Bowers $S = 1/2$ dimer model. In compound **1** the presence of an additional V^{IV} connected with the V^{IV} dimers through $\mu_{1,2}$-PO_4^{3-} bridges is described with a Curie–Weiss type correction. This model reproduces the magnetic properties of compound **1** with $g = 1.956$, $J_{dim} = -102.1\ cm^{-1}$, $\theta = -0.4\ cm^{-1}$ and $N\alpha = 278 \times 10^{-6}$ emu mol^{-1}. In compound **2**, the presence of a small percentage of paramagnetic impurity has to be considered to account for the divergence of χ_m at low temperatures. This simple model reproduces the magnetic data of compound **2** with $g = 1.99$, $J = -62.4\ cm^{-1}$ and a 1.2% of monomeric impurity. The moderate antiferromagnetic coupling found in the triply oxido bridges V^{IV} dimers is justified from the structural parameters of the bridge. These studies confirm that the coupling through –O–P–O– bridges is antiferromagnetic and relatively weak, as well as previous magneto-structural correlations in this kind of oxido bridges. DFT calculations on a dinuclear fragment model for the two systems gave the following values of $J_{calc} = -72.4\ cm^{-1}$ for **1** and $J_{calc} = -5.2\ cm^{-1}$ for **2**. These values reproduce the antiferromagnetic nature of the superexchange interactions between the V^{IV} centers.

1. Introduction

Vanadium phosphorus oxides (VPO) are studied due to the great structural variety they can present. The wide number of structures that can be obtained by the different combinations of the vanadium polyhedra with the phosphorus polyhedra, range from 0D to 3D crystalline lattices. Moreover, vanadium can present different oxidation states; this fact confers more plasticity and more variety to these inorganic lattices. Besides, the use of organic ligands offers the possibility to direct and modulate the dimensionality and coordination modes in these VPO systems, giving rise to the so-called hybrid organic–inorganic compounds.

Magnetic properties of inorganic lattices based on VPO systems may depend on the structural features of the inorganic network, and on the nature of the paramagnetic centers present in the structure. In the specific case of V^{IV}-based VPO systems, these are interesting because the vanadium spin carrier is directly condensed into the VPO network. The phosphate bridges of oxovanadium phosphates are known to provide spin exchange pathways, and the way these bridges are coordinated determines the magnitude of the superexchange interaction between the paramagnetic V^{IV} centers [1–7]. However, in a 1D or 2D structure the different bonding modes of the phosphate groups to the vanadium atoms do not permit to unambiguously assign the magnitude of the spin exchange interaction related to the different magnetic exchange pathways present in the structure. Besides, the intrachain interactions in oxovanadium phosphate bridged chains have been shown to be stronger than the interchain ones [8].

At present, chemists are able to prepare in a reproducible manner and in quantitative yields different VPO phases and the corresponding functionalized MVPO systems by hydrothermal synthetic methods. Therefore they are able to obtain large amounts

* Corresponding author at: Facultad de Química y Biología, Universidad de Santiago de Chile (USACH), Chile. Tel.: +562 7181079; fax: +562 6812108.
E-mail address: diego.venegas@usach.cl (D. Venegas-Yazigi).

0020-1693/$ - see front matter © 2012 Elsevier B.V. All rights reserved.
http://dx.doi.org/10.1016/j.ica.2012.10.024

of pure solids in order to measure their physical properties [9–14]. In this work we have measured the bulk magnetic properties of two vanadium(IV) extended systems, and used molecular magnetism models to fit these data, and explain the observed magnetic behavior. Theoretical calculations based on Density Functional Theory were used to explain the antiferromagnetic nature of the experimental magnetic data.

2. Experimental

2.1. Synthesis

A mixture of V_2O_5, $NaVO_3{\cdot}H_2O$, 2,2′-bipyridine, $NH_2OH{\cdot}HCl$, H_3PO_4 and H_2O in a molar ratio of 0.55 (100 mg):1.5 (182 mg): 1.5 (234 mg):5.0 (347.5 mg):6.5 (0.3725 mL):1000 (18 mL) were added to a Parr reactor and heated at 200 °C for 96 h. Two phases were obtained, which were separated mechanically: green crystals of $[(VO)_3(\mu_5\text{-}PO_4)_2(2,\acute{2}\text{-bpy})(\mu\text{-}OH_2)]{\cdot}1/3H_2O$ (**1**) (52.1% yield), and as minor product blue crystals of $(VO)_2H_4P_2O_9$ (**2**) (less than 4% yield).

An alternative synthetic method was used to obtain a better yield of compound (**2**). While all amounts of the reagents were reduced, the relative amount of the reducing agent $NH_2OH{\cdot}HCl$, was increased. A mixture of V_2O_5, $NaVO_3{\cdot}H_2O$, 2,2′-bipyridine, $NH_2OH{\cdot}HCl$, H_3PO_4 and H_2O in a molar ratio of 0.27 (50 mg):0.75 (91 mg):0.75 (117 mg):4 (278 mg):3.25 (0.1862 mL):1000 (18 mL) mmol with a reaction time of 96 h; the cooling time was 48 h. With these modifications the yield of (**2**) increased (80.8% yield), and larger crystals of (**2**) were obtained.

Both compounds were identified by their powder diffraction patterns; compound (**1**): trigonal, space group *R*3, $a = 29.7600(3)$ Å, $c = 9.5745(2)$ Å; compound (**2**): orthorhombic, space group *Pmmm*, $a = 7.416(1)$ Å, $b = 9.592(2)$ Å, $c = 5.689$ Å. These crystalline parameters were previously reported by Yang and Lu [13] and Torardi and Calabrese [14], respectively.

3. Magnetic study

3.1. Experimental

The DC magnetic susceptibility measurements were carried out in the temperature range 2–300 K with applied magnetic fields of 0.1 and 1.0 T on polycrystalline samples of compounds **1** and **2** (with masses of 36.23 and 25.92 mg, respectively) with a Quantum Design MPMS-XL-5 SQUID susceptometer. The isothermal magnetizations were performed on the same samples at 2 K with magnetic fields up to 5 T. The susceptibility data were corrected for the sample holders previously measured using the same conditions and for the diamagnetic contributions of the salts as deduced by using Pascal's constants ($\chi_{dia} = -147.78 \times 10^{-6}$ and -137.76×10^{-6} emu mol^{-1} for **1** and **2**, respectively) [15].

3.2. Computationals details

Single point calculations were performed using a fragment generated from the crystalline structure containing two vanadium atoms. Spin-unrestricted calculations under the Density Functional Theory approach were done, using the hybrid B3LYP functional [16] and a triple-ζ all electron basis set for all atoms [17]. A guess function was generated using Jaguar 5.5 code [18], and a triple-ζ basis set was used for all the atoms. Total energy calculations were performed with the GAUSSIAN09 program [19], using the quadratic convergence method with a convergence criterion of 10^{-7} a.u. Mulliken spin densities were also obtained from the single point calculations.

The Heisenberg–Dirac–van Vleck spin Hamiltonian was used to describe the exchange coupling in the polynuclear complex:

$$\hat{H} = -\sum_{i>j} J_{ij} S_i S_j$$

where, S_i and S_j are the spin operators of the paramagnetic centers *i*, *j* of the compound. The J_{ij} parameters are the magnetic coupling constants between the centers with unpaired electrons of the molecule.

4. Results and discussion

4.1. Magnetic study for $[(VO)_3(\mu\text{-}PO_4)_2(2,2'\text{-bpy})(\mu\text{-}OH_2)]{\cdot}1/3H_2O$ (*1*)

The experimental magnetic behavior of **1** is shown in Fig. 1. The product of the molar magnetic susceptibility times the temperature, $\chi_m T$ per V^{IV} trimer, shows a room temperature value of ca. 1.06 emu K mol^{-1} (close to 1.125 emu K mol^{-1}, the expected value for three isolated $S = 1/2$ V^{IV} centers with $g = 2.00$). On lowering the temperature, $\chi_m T$ shows a progressive decrease to reach a plateau with a value of ca. 0.35 emu K mol^{-1} in the temperature range 20–5 K. Below ca. 5 K $\chi_m T$ shows an abrupt decrease to reach a value of ca. 0.26 emu K mol^{-1} at 2 K.

This behavior indicates that the three $S = 1/2$ V^{IV} centers present predominantly antiferromagnetic interactions that cancel the contribution of two of the three V^{IV} centers since the plateau observed at low temperatures (ca. 0.35 emu K mol^{-1}) corresponds to the expected value for one unpaired electron (0.375 emu K mol^{-1} for $g = 2$). The more abrupt decrease observed at very low temperatures suggests the presence of an additional and weaker antiferromagnetic coupling present in the remaining unpaired electron.

The isothermal magnetization M(H) at 2 K shows a saturation value slightly lower than 1.0 μ_B, which is the theoretical saturation value for a $S = 1/2$ ground state with $g = 2.00$. This lower value confirms the presence of the additional weak antiferromagnetic coupling observed at very low temperatures.

In order to fit the magnetic data we have to analyze the possible magnetic exchange pathways in the structure of compound **1**. As can be seen in Fig. 2, this compound presents a V^{IV} dimer where the two vanadium atoms, V2 and V3, are connected through a triple oxido bridge from two short $\mu_{1,1}\text{-}PO_4$ bridges (V2–O4 = 2.089(3), V2–O7 = 2.073(3), V3–O4 = 2.040(3) and V3–O7 = 2.025(3) Å) and one long water bridge (V2–O12 = 2.463(3) and V3–O12 = 2.459(3) Å).

Each V^{IV} center of the dinuclear unit presents a distorted VO_6 octahedral geometry where the equatorial plane is formed by four

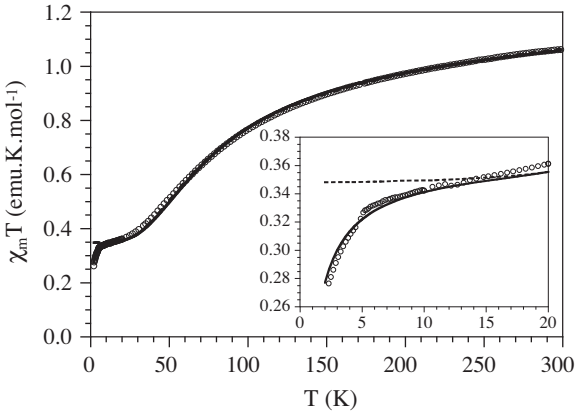

Fig. 1. Thermal variation of the $\chi_m T$ product of compound **1**. Solid and dashed lines are the best fits to the models (see text). Inset shows the low temperature region.

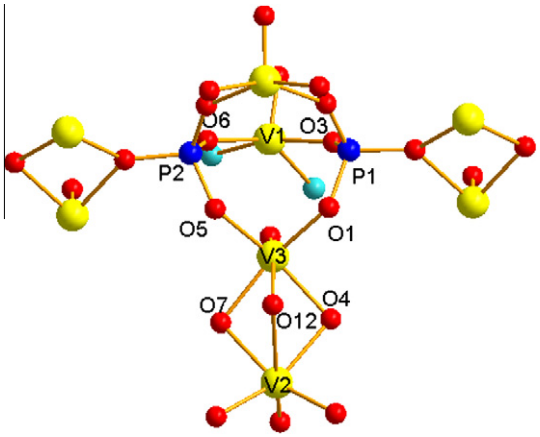

Fig. 2. Coordination environment and bridges between the V atoms in compound **1**. color code: V1, V2, V3 = yellow, P = blue, O = red, N = light blue. (For interpretation of the references to color in this figure legend, the reader is referred to the web version of this article.)

oxygen atoms from four different PO_4^{3-} groups and the axial positions are occupied by a water molecule (O12) and a terminal oxygen atom with a very short bond length (corresponding to a vanadyl group). Besides this $(\mu\text{-O})_3$ V^{IV} dimer, there is an additional V^{IV} atom (V1) which is connected to four different V2–V3 dimers through $\mu_{1,2}$-PO_4 bridges (Fig. 2). These connections are not identical in the four dimers. Thus, V1 is connected through a single –O–P–O– bridge with the two V atoms of two neighboring dimers and through a double –O–P–O– bridge and with only one V atom of two more dimers.Since the –O–P–O– bridges are known to give rise to much weaker coupling than a direct oxido bridge, we have considered, in a first approach, that these $\mu_{1,2}$-PO_4 bridges are negligible and, accordingly, we have used a very simple $S = 1/2$ dimer model plus an additional $S = 1/2$ paramagnetic contribution to account for the magnetically almost isolated V1 atom. The Hamiltonian used for the intra-dinuclear interaction is: $\hat{H} = -J(\hat{S}_1 \cdot \hat{S}_2)$ and we have used the expression derived for the susceptibility by Bleaney and Bowers [20], plus an additional paramagnetic $S = 1/2$ term and a temperature independent paramagnetic term ($N\alpha$):

$$\chi = \frac{2N\beta^2 g^2}{kT} \cdot \frac{1}{3 + \exp(-J/kT)} + \frac{N\beta^2 g^2}{4kT} + N\alpha$$

This simple equation reproduces quite satisfactorily the magnetic properties of compound **1** in the temperature range 5–300 K with the following parameters: $J_{dim} = -99.2\ cm^{-1}$, $g_{dim} = g_{mon} = 1.923$ and $N\alpha = 382 \times 10^{-6}$ emu mol^{-1} (dashed line in Fig. 1). Note that at very low temperatures the agreement between the experimental points and the calculated ones is not good since the experimental data show an abrupt decrease below ca. 5 K that is not reproduced by the used model (inset in Fig. 1) since the calculated $\chi_m T$ values remain constant, as expected for an isolated $S = 1/2$ center.

In order to reproduce the low temperature decrease observed in compound **1**, we have to include the coupling between the monomer V1 and the dimers through the $\mu_{1,2}$-PO_4^{3-} bridges. Albeit, the inclusion of all these interactions, leads to an extended 2D magnetic pathway with a closed curvature that generates the tubular structure observed in compound **1**. Since there is no available magnetic model to fit such structure, we have used a very simple model with an additional interaction by including in the previous model a temperature correction of the $(T - \theta)$ type, as in the Curie–Weiss law.

This simple model reproduces much better the magnetic properties of compound **1**, including the decrease at very low temperatures, with $g = 1.956$, $J_{dim} = -102.1\ cm^{-1}$, $\theta = -0.4\ cm^{-1}$ and $N\alpha = 278 \times 10^{-6}$ emu mol^{-1} (solid line in Fig. 1). As expected, the intra-dimer coupling constant is similar to the one found in the first model since the weak additional interaction (θ) has almost no influence on the high temperature region and only affects the low temperature data.

The magnetic couplings found in the two models agree with the nature of the corresponding bridges. Thus, in the triply oxido-bridged V^{IV} dimer, the V2–O4–V3 and V2–O7–V3 bond angles connecting equatorial positions (96.13(11)° and 97.10(11)°, respectively) are in the normal range where strong antiferromangetic interactions are calculated and observed [21]. Although there is an oxido bridge with a V2–O12–V3 angle of 77.23(9), which is expected to produce a ferromagnetic coupling, this bridge connects axial positions of both V atoms and, therefore it is expected to give a very reduced magnetic coupling since the magnetic orbitals are located in the equatorial plane. Furthermore, the coupling is weak since the V2–O12 and V3–O12 bond lengths are very long (2.463(3) and 2.459(3) Å, respectively). On the other hand, the magnetic coupling found in both phosphate bridges is weak and antiferromagnetic, as observed in other similar V^{IV} compounds with this kind of bridge [22–25]. Independently of the used model, the magnetic properties of compound **1** are clearly dominated by the strong antiferromagnetic coupling through the three oxido bridges inside the face-sharing V^{IV} dimer, which is much stronger than the other phosphate-bridged couplings.

4.2. Magnetic study of $(VO)_2H_4P_2O_9$ (**2**)

The thermal variation of the molar magnetic susceptibility per V^{IV} dimer, shows an increase when the temperature is decreased and reaches a maximum at ca. 57 K (Fig. 3). Below this temperature χ_m decreases and reaches a minimum at ca. 10 K followed by a divergence at lower temperatures. The presence of a maximum in the χ_m versus T plot suggests the presence of predominant antiferromagnetic exchange interactions in compound **2**. The divergence observed at low temperatures in the form of a Curie-tail indicates the presence of paramagnetic impurities as a consequence of crystal defects, vacancies and/or monomeric inclusion impurities.

The structure of compound **2** shows layers containing octahedral V^{IV} atoms arranged in face-sharing dimers connected through a triple oxido bridge (Fig. 4, left). Each dimer is further connected to its six closest neighboring dimers through double –O–P–O– bridges to form a rhombic 2D lattice (Fig. 4, right).

Accordingly, in order to fit the magnetic properties of compound **2** we have used a simple Bleaney–Bowers $S = 1/2$ dimer model [20] with a paramagnetic $S = 1/2$ impurity to reproduce the increase in χ_m at low temperatures:

$$\chi = (1 - \rho)\frac{2N\beta^2 g^2}{kT}\frac{1}{3 + \exp(-J/kT)} + \rho\frac{N\beta^2 g^2}{4kT}$$

This simple model reproduces very satisfactorily the magnetic properties of compound **2** in the whole temperature range with the following parameters: $g = 1.99$, $J = -62.4\ cm^{-1}$ and $\rho = 1.2\%$ (solid line in Fig. 3). Note that although the interdimer exchange interactions through the double –O–P–O– bridges have been neglected, the good agreement between the experimental and calculated plots confirms that these phosphate bridges can be neglected as compared to the triple oxido bridge inside the V^{IV} dimers. This assumption is also confirmed by the fact that in compound **1** the coupling through the –O–P–O– bridges was very weak and its effect is expected to be noticed only at low temperatures, where the paramagnetic impurity is predominant.

In compound **2**, as also observed in compound **1**, the intra-dimer antiferromagnetic exchange interaction is quite strong and

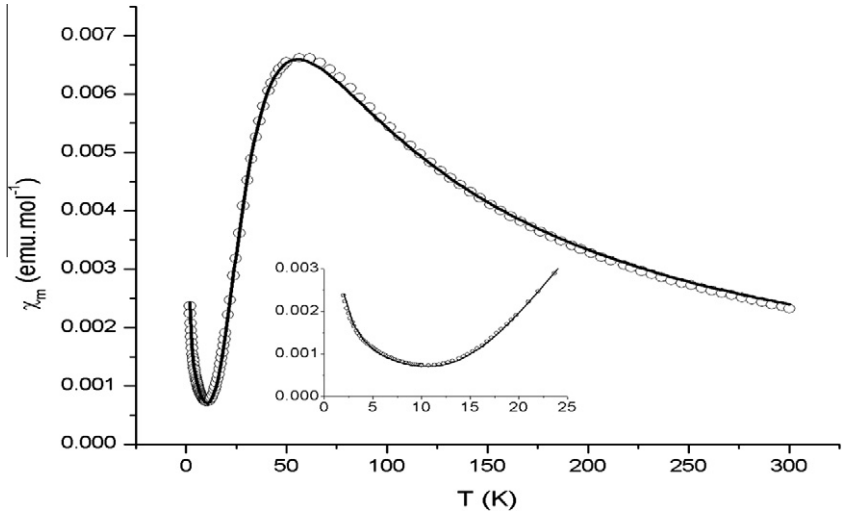

Fig. 3. Thermal variation of the magnetic susceptibility of compound **2** per V^{IV} dimer. Inset shows the low temperature region.

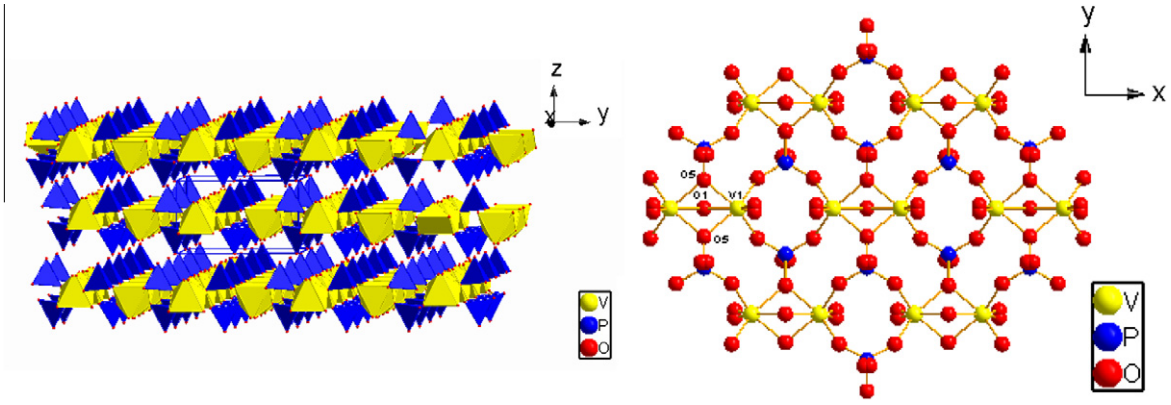

Fig. 4. (Left) Layered structure of compound **2**. (Right) View of one layer showing a central dimer surrounded by six dimers. Color code: V = yellow, P = blue, O = red. (For interpretation of the references to color in this figure legend, the reader is referred to the web version of this article.)

can be easily correlated with the presence of the triple oxido bridge with one V–O_w–V bridging angle of 82.98° and two V–O(PO_3)–V angles of 97.30°. This last value is very similar to the values observed in compound **1** and is also in the normal range where strong antiferromangetic interactions are calculated and observed [21]. Although there is an additional small V–O_w–V bond angle (corresponding to the water molecule), this bridge is expected to originate a very weak magnetic coupling since the V–O bond lengths in this bridge are very long (V1–O1 = 2.336 Å).

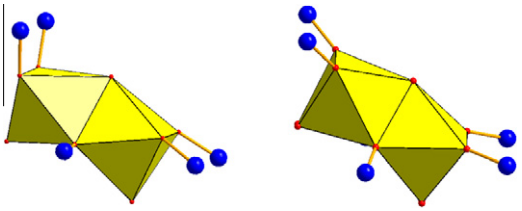

Fig. 5. Polyhedral representation of the dinuclear unit of **1** (left) and 2 (right).

4.3. Theoretical calculations

If we compare the structures of **1** and **2**, it is possible to observe a distortion in both structures with respect to the vanadium polyhedra of the dinuclear units as can be seen in Fig. 5.

In order to describe in a more detailed way the magnetic phenomena, DFT calculations were performed for systems **1** and **2**, on a model that considers two isolated paramagnetic centers. Since the Kahn–Briat model establishes a direct correlation between the overlap of the magnetic orbitals and the strength of the superexchange phenomena, the overlap of the magnetic orbitals was calculated and shows that for **1** the overlap is $S_{ab}{}^2 = 0.002$ and for **2** it is $S_{ab}{}^2 = 0.014$. Both dinuclear units can be described as two octahedra sharing one face, but the overlap of the magnetic orbitals is shown to be different and therefore generating different intensity of the exchange phenomena for **1** and **2**.

Even though the theoretical calculations of the magnetic exchange constants for **1** and **2** reproduce the antiferromagnetic nature of the magnetic phenomena observed for the two systems, the obtained values are lower. This is due to the use of a simple structural dinuclear model. These calculations gave the following values for the super exchange interactions $J_{calc} = -72.4\ cm^{-1}$ for **1** and $J_{calc} = -5.2\ cm^{-1}$ for **2**, corroborating the tendency observed experimentally.

The Mulliken spin density values were determined for the two model structures of **1** and **2,** in order to validate the calculated electronic structures. The values for the V^{IV} atoms obtained in the calculation for the two models are shown in Table 1S. All the calculated values are in the range of 1.19e− to 1.23e−, as obtained for other studied V^{IV} systems [26]. The spin density is located on

the metal centers, and part of this density appears over the oxygen atoms of the vanadyl group, which occurs due to a polarization mechanism. Figs. S1 and S2 present the spin density surfaces for the ferromagnetic solution $S_T = 1$ and the broken-symmetry solution $S_T = 0$ for **1** and **2**, respectively.

5. Conclusions

We have shown that it is possible to explain and fit the magnetic properties of two different vanadium phosphates containing V^{IV} dimers connected through triple oxido bridges, which are further connected through μ_{12}-PO_4^{3-} bridges. The magnetic coupling in these two compounds has been reproduced with a simple $S = 1/2$ dimer model plus a $S = 1/2$ monomer contribution in compound **1,** and a paramagnetic $S = 1/2$ impurity in compound **2**. To reproduce the decrease observed in the $\chi_m T$ product at very low temperatures in compound **1** we have included a weak temperature correction term. The couplings found in both compounds show that the triple oxido bridges give rise to strong antiferromagnetic interactions ($J = -102.1$ and $-62.4\ cm^{-1}$ in **1** and **2**, respectively), whereas the coupling through the phosphate bridges is very weak in compound **1** and negligible in compound **2** (compared with the contribution of the paramagnetic impurity). Finally the sign and relative relevance of the exchange pathways were confirmed by DFT calculations.

Acknowledgments

The authors thank FONDECYT 1080316 and Financiamiento Basal Program FB0807 for partial financial support. Authors acknowledge ECOS-CONICYT C08E02 International Project. This work was done under the LIA-MIF CNRS 836 Collaborative Program. We also acknowledge the Spanish Ministerio de Economía y Competitividad (Projects Consolider-Ingenio 2010 CSD 2007-00010 and CTQ2011-26507) and the Generalitat Valenciana (Prometeo Program). M.S. thanks CONICYT for the 21050162 and AT-24071044 doctoral scholarships. W.C.M. thanks CONICYT for Doctoral Scholarships (21080445 and AT24100006).

Authors also thank Powered@NLHPC: This research was partially supported by the supercomputing infrastructure of the NLHPC (ECM-02), Centre for Mathematical Modeling CMM, Universidad de Chile.

Appendix A. Supplementary material

Supplementary data associated with this article can be found, in the online version, at http://dx.doi.org/10.1016/j.ica.2012.10.024.

References

[1] P. Amoros, A. Beltrán, D. Beltrán, J. Alloys Comp. 188 (1992) 123.
[2] M. Roca, P. Amoros, J. Cano, M.D. Marcos, J. Álamo, A. Beltran-Porter, D. Beltran-Porter, Inorg. Chem. 37 (1998) 3167.
[3] D. Venegas-Yazigi, K. Muñoz-Becerra, E. Spodine, K. Brown, C. Aliaga, V. Paredes-García, P. Aguirre, A. Vega, R. Cardoso-Gil, W. Schnelle, R. Kniep, Polyhedron 29 (2010) 2426.
[4] E. Spodine, D. Venegas-Yazigi, S. Ushak, V. Paredes-García, M. Saldías, E. Le Fur, J.-Y. Pivan, Polyhedron 26 (2007) 2121.
[5] S. Ushak, E. Spodine, E. Le Fur, D. Venegas-Yazigi, J.-Y. Pivan, W. Schnelle, R. Cardoso-Gil, R. Kniep, Inorg. Chem. 45 (2006) 5393.
[6] Y. Moreno, A. Vega, S. Ushak, R. Baggio, O. Pena, E. Le Fur, J.-Y. Pivan, E. Spodine, J. Mater. Chem. 13 (2003) 2381.
[7] S. Ushak, E. Spodine, D. Venegas-Yazigi, E. Le Fur, J.-Y. Pivan, O. Pena, R. Cardoso-Gil, R. Kniep, J. Mater. Chem. 15 (2005) 4529.
[8] H.J. Koo, M.H. Whangbo, Inorg. Chem. 39 (2000) 3599.
[9] E. Le Fur, O. Peña, J.Y. Pivan, J. Mater. Chem. 12 (2002) 132.
[10] E. Le Fur, J.Y. Pivan, J. Solid State Chem. 158 (2001) 94.
[11] E. Le Fur, J.Y. Pivan, J. Mater. Chem. 9 (1999) 2589.
[12] E. Le Fur, O. Peña, J.Y. Pivan, J. Alloys Comp. 285 (1999) 89.
[13] W. Yang, C. Lu, Inorg. Chem. 41 (2002) 5638.
[14] C.C. Torardi, J.C. Calabrese, Inorg. Chem. 23 (1984) 1310.
[15] G.A. Bain, J.F.J. Berry, Chem. Educ. 85 (2008) 532.
[16] A.D. Becke, J. Chem. Phys. 98 (1993) 5648.
[17] A. Schaefer, C. Huber, R. Ahlrichs, J. Chem. Phys. 100 (1994) 5829.
[18] JAGUAR, version 5.5, Schrödinger, LLC, Portland, OR, USA, 2003.
[19] M.J. Frisch et al., GAUSSIAN 09 (Revision D.2), GAUSSIAN Inc., Pittsburgh, PA, USA, 2009.
[20] B. Bleaney, K.D. Bowers, Proc. R. Soc. Lond. Ser. A 214 (1952) 451.
[21] E. Ruiz, P. Alemany, S. Alvarez, J. Cano, J. Am. Chem. Soc. 119 (1999) 1297.
[22] X.M. Zhang, H.S. Wu, S. Gao, X.M. Chen, J. Solid State Chem. 176 (2003) 69.
[23] J. Do, R.P. Bontchev, A.J. Jacobson, J. Solid State Chem. 154 (2000) 514.
[24] B. Koo, W. Ouellette, E.M. Burkholder, V. Golub, C.J. O'Connor, J. Zubieta, Solid State Sci. 6 (2004) 461.
[25] W. Chang, S. Wang, Chem. Mater. 17 (2004) 74.
[26] L. Zhang, Z. Chen, Chem. Phys. Lett. 345 (2001) 353.